

## N O T I C E

THIS DOCUMENT HAS BEEN REPRODUCED FROM  
MICROFICHE. ALTHOUGH IT IS RECOGNIZED THAT  
CERTAIN PORTIONS ARE ILLEGIBLE, IT IS BEING RELEASED  
IN THE INTEREST OF MAKING AVAILABLE AS MUCH  
INFORMATION AS POSSIBLE



Technical Memorandum 80328

80328

# The Relationship of Red and Photographic Infrared Spectral Data to Grain Yield Variation Within a Winter Wheat Field

Compton J. Tucker,  
Brent N. Holben, James H. Elgin, Jr.,  
and James E. McMurtrey III

(NASA-TM-80328) THE RELATIONSHIP OF RED AND  
PHOTOGRAPHIC INFRARED SPECTRAL DATA TO GRAIN  
YIELD VARIATION WITHIN A WINTER WHEAT FIELD  
(NASA) 26 p HC A03/MF A01

CSCL 02C

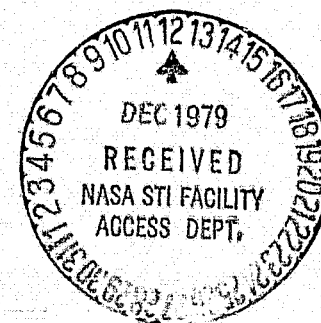
N80-12532

G3/43 Unclassified 41471

JULY 1979

National Aeronautics and  
Space Administration

Goddard Space Flight Center  
Greenbelt, Maryland 20771



TM 80318

THE RELATIONSHIP OF RED AND PHOTOGRAPHIC  
INFRARED SPECTRAL DATA TO GRAIN YIELD  
VARIATION WITHIN A WINTER WHEAT FIELD\*

Compton J. Tucker  
Brent N. Holben  
Earth Resources Branch  
NASA Goddard Space Flight Center  
Greenbelt, Maryland 20771 USA

James H. Elgin, Jr.  
James E. McMurtrey III  
Beltsville Agricultural Research Center  
Field Crops Laboratory  
Plant Genetics and Germplasm Institute  
USDA/SEA/AR  
Beltsville, Maryland 20705 USA

July 1979

\*This is a preprint of a manuscript submitted to Photogrammetric Engineering and Remote Sensing

GODDARD SPACE FLIGHT CENTER  
Greenbelt, Maryland 20771

**Page intentionally left blank**

**THE RELATIONSHIP OF RED AND PHOTOGRAPHIC  
INFRARED SPECTRAL DATA TO GRAIN YIELD  
VARIATION WITHIN A WINTER WHEAT FIELD**

**ABSTRACT**

Two-band hand-held radiometer data from a winter wheat field, collected on 21 dates during the spring growing season, were correlated with within field final grain yield. Significant linear relationships were found between various combinations of the red and photographic infrared radiance data collected and the grain yield. The spectral data explained ~64% of the within field grain yield variation. This variation in grain yield could not be explained using meteorological data as these were similar for all areas of the wheat field. Most importantly, data collected early in the spring were highly correlated with grain yield; a five-week time window existed from stem elongation through antheses in which the spectral data were most highly correlated with grain yield; and manifestations of wheat canopy water stress were readily apparent in the spectral data.

**Page intentionally left blank**

## **CONTENTS**

	<u>Page</u>
<b>BACKGROUND .....</b>	1
<b>DESCRIPTION OF RESEARCH UNDERTAKEN .....</b>	2
<b>EXPERIMENTAL PROCEDURE .....</b>	3
<b>RESULTS AND DISCUSSION .....</b>	6
<b>CONCLUSIONS .....</b>	19
<b>ACKNOWLEDGMENTS .....</b>	19
<b>REFERENCES .....</b>	20

## THE RELATIONSHIP OF RED AND PHOTOGRAPHIC INFRARED SPECTRAL DATA TO GRAIN YIELD VARIATION WITHIN A WINTER WHEAT FIELD

### BACKGROUND

REPRODUCIBILITY OF THE  
ORIGINAL PAGE IS POOR

Several approaches for remote sensing of winter wheat yield have been proposed. The Large Area Crop Inventory Experiment (LACIE) involving NASA, NOAA, and the USDA, was perhaps the most visible and the best known of various winter wheat yield prediction approaches. Simulation or regression models were used to predict wheat yield based upon climatic conditions (MacDonald and Hall, 1977).

The EarthSat Corp. (1976) has proposed a spring wheat yield prediction method. This approach differs from the LACIE approach in that NOAA meteorological satellite data were used to estimate grid cell precipitation which in turn drove the yield determination. Critical variables for this approach were the calculation of soil moisture and grid cell weather from the meteorological satellite data and the determination of crop phenology (LACIE, 1978).

Idso et al. (1977a,b) have proposed a method of winter wheat yield prediction using the stress degree day concept. That is, the final yield of a crop was hypothesized to be linearly related to the accumulated stress degree days over some critical period. This technique was developed in Phoenix, Arizona under irrigated conditions and is currently being evaluated in dryland winter wheat growing areas.

Hammond (1975) and Morain and Williams (1975) have discussed monitoring wheat production with satellite remotely sensed data. Harlan and Liu (1975) and Colwell et al. (1977) have evaluated the use of Landsat data for inferring direct winter wheat grain yield predictions. Spectral data were used to estimate yield related variables such as stand density or leaf area index. Because grain yield is usually highly correlated to stand density or leaf area index, a direct estimate of final grain yield was usually possible. Colwell et al. (1977) concluded that Landsat (i.e., spectral) data explained a

considerable amount of yield variation which was not explained by meteorological data. In addition, Landsat derived yield predictions were as highly correlated with individual field yields as were estimates made using traditional sampling techniques, even, in some cases, if the Landsat data were collected several weeks before the field samples.

Heilman et al. (1977) reported a technique for estimating winter wheat grain yields using Landsat derived estimates of leaf area index coupled with an evapotranspiration model. More recently, Wiegand et al. (1979) discussed leaf area index estimates for winter wheat made from Landsat data and the implications for evapotranspiration and crop simulation modeling using these data.

Accurate inputs for crop canopy leaf area index are a necessity for successful evapotranspiration and crop simulation modeling. To achieve accurate leaf area index estimates from Landsat data, "ground-truth" sampling must occur which adequately samples the variability of the actual field leaf area index for enough Landsat pixels ( $\sim 0.45$  ha) to satisfy basic sampling theory requirements. This has often proven difficult to achieve. Heilman et al. (1977), Kanemasu et al. (1977), and Wiegand et al. (1979) all used three ground samples of 91 cm by 2 row widths ( $\sim 40$  cm) to establish each field's ( $>40$  ha) leaf area index. Thus  $\sim 1$  m<sup>2</sup> was used to determine the leaf area index of a large field. This could be a significant source of error for the evapotranspiration and crop yield modeling approaches (Wiegand et al., 1979). "Ground-truth" sampling must adequately account for the in situ population variability by inclusion of enough samples to allow for a reasonable estimate of the actual field leaf area index.

#### DESCRIPTION OF RESEARCH UNDERTAKEN

As part of an ongoing research program into future satellite sensor development including selection and evaluation of spectral bands, radiometric resolution, frequency of coverage, orbit selection, and other considerations for vegetational applications, we have been collecting hand-held radiometer data from a variety of agricultural crops in a NASA/GSFC-USDA/BARC cooperative research program. Previous research on alfalfa, corn, and soybeans had demonstrated that red and photographic infrared two-band radiometer data were highly correlated with various properties of plant canopies (Tucker et al., 1979a,b,c). Therefore, we decided to evaluate the applicability of these data for yield predictions

on wheat. A companion paper reports on the use of these same data for monitoring total dry matter accumulation (Tucker et al., 1979d).

Previous work with the green leaf or photosynthetically active biomass has suggested that this physiological entity integrated the various biotic and abiotic effects present in the plant canopies (Tucker et al., 1973; Colwell et al., 1977; Tucker et al., 1979a,b). Conditions which adversely affected plant growth and development resulted in a reduction in the photosynthetically active biomass. Because the photosynthetically active biomass or green leaf area is one of the basic system variables in primary production, monitoring this system variable throughout the growing season should enable inferences to be made regarding total dry matter accumulation and grain yield. This has been proposed as the Leaf Area Duration (LAD) concept (Colwell et al., 1977; Richardson et al., 1979).

However, the LAD concept needs to be modified in that the photosynthetically active biomass or leaf area is actually the interaction between the green LAI and the chlorophyll concentration. Expressed in other words, the photosynthetically active biomass can be defined as the interaction between inter- and intra-leaf scattering and chlorophyll absorption which occurs predominately in the green leaves of the plant canopy in question.

Red and photographic infrared spectral data have been demonstrated by many workers to be highly correlated with the photosynthetically active biomass of several cover types (reviewed in Tucker, 1979). The red spectral data are highly correlated with the *in vivo* chlorophyll concentration, whereas the photographic infrared data are highly correlated with LAI. Thus, various linear combinations of these two adjacent spectral regions are highly related to the photosynthetically active biomass (Tucker, 1979).

REPRODUCIBILITY OF THE  
ORIGINAL PAGE IS POOR

#### EXPERIMENTAL PROCEDURE

Our experiment was conducted in a 1.2-ha soft red winter wheat (Triticum aestivum L.) field at the Beltsville Agricultural Research Center, Beltsville, Maryland. The field was plowed, disked, and planted with the cultivar 'Arthur' on October 6, 1977 at a rate of 107.6 kg/ha. A conventional grain drill with 17.8-cm row spacing was used for seeding. Before seeding the field was limed on the

basis of soil test recommendations and fertilizer was applied at a rate of 33.3 kg N, 53.8 kg P, and 53.8 kg K/ha. The following spring (early March 1978) the crop was topdressed with 20.4 kg N/ha.

Twenty 2- x 3-m plots were selected during the winter dormant period in the wheat field. Subsequently, for each plot, four pairs of red (0.65-0.70  $\mu\text{m}$ ) and photographic infrared (0.775-0.825  $\mu\text{m}$ ) spectral radiance measurements were obtained using a hand-held digital radiometer (Pearson et al., 1976) on 21 dates between March 21, 1978 (Julian date 80) and June 23, 1978 (Julian date 174). The intervals between dates ranged from 1 to 9 days; however, the average interval was 4.7 days and the median interval was a tie between four and five days (Table 1).

The red and photographic infrared spectral radiance data were used to form the ir/red ratio and the normalized difference (ND) of Rouse et al. (1973) and Deering et al. (1975) where:

$$\text{ND} = (\text{IR} - \text{RED}) / (\text{IR} + \text{RED}) \quad (1)$$

The four pairs of the spectral measurements per plot were averaged to account for the spatial variability present in each plot. All spectral data were collected plus or minus 90 minutes of local solar noon, measured normal to the ground surface at a height of  $\sim 1$  m above the plant canopy under sunny skies (Table 1).

Throughout the growing season average plant height, percentage cover estimates, and phenological development notes were recorded for the field area (Table 2). The crop reached harvest maturity in late June 1978. On June 28, 1978 (Julian date 179) a 0.9- x 3.0-m swath was cut with a small sickle bar mower from the center of each plot and the grain thrashed with a small plot grain thrasher. The grain yields were oven dried at 60°C for 72 hours and were subsequently adjusted to 14% moisture and expressed in g/m<sup>2</sup>.

A regression approach was taken in which the average red radiance, ir radiances, ir/red ratio, and ND were correlated with the grain yield for each of the 21 data collection dates. In addition, the ir/red ratio and the ND as a function of Julian date and growing degree days were integrated for four different time intervals and correlated with grain yield.

REPRODUCIBILITY OF THE  
ORIGINAL PAGE IS POOR

Table 1  
Tabular Listing of the Days when Hand-Held Radiometer Data Were Collected  
from the 20 2 x 3 m Winter Wheat Plots in 1978

Sampling Sequence	Julian Date	Time (EST)	Conditions/Comments (Temperature, Sky, Wind, Etc.)
1	80	1130-1215	12°C, clear with no clouds, wind = 16 kmh
2	89	1215-1300	8°C, clear with no clouds, calm, soil damp
3	92	1222-1310	15°C, clear with no clouds, calm
4	95	1220-1245	17°C, a few scattered clouds, wind = ~5-10 kmh
5	97	1225-1247	21°C, a few scattered clouds, calm
6	102	1110-1135	14°C, clear with no clouds, wind = ~5 kmh
7	104	1210-1230	20°C, clear with no clouds, wind = 30-45 kmh
8	112	1338-1415	18°C, scattered clouds, gusty wind = 5-20 kmh
9	118	1230-1310	22°C, clear with no clouds, gusty wind = 5-30 kmh
10	121	1200-1230	16°C, clear with no clouds, wind = 5-10 kmh
11	123	1215-1250	18°C, clear with no clouds, calm
12	131	1145-1210	24°C, a few scattered clouds, wind = ~10 kmh
13	139	1145-1230	20°C, a few scattered clouds, wind = <15 kmh
14	146	1125-1205	19°C, a few scattered clouds, calm
15	152	1130-1200	22°C, clear with no clouds, wind = 5-10 kmh, plots 33-35 crushed by animals (deer?)
16	157	1050-1120	22°C, a few scattered clouds, wind = ~10 kmh
17	161	1230-1300	26°C, clear with no clouds, calm, plots 23-35 lodged
18	165	1030-1125	17°C, a few scattered clouds, wind = 25-40 kmh
19	166	1100-1200	20°C, high faint cirrus, calm, bird damage to plots 21-40
20	170	1030-1100	20°C, a few scattered clouds, wind = <10 kmh
21	174	1100-1130	28°C, clear with no clouds, calm

Mean time between sampling dates = 4.7 days

Range between sampling dates = 1-9 days

Medium time between sampling dates = 4.5 days (tie)

**Table 2**  
**Agronomic Data Pertaining to Average Plant Heights, Estimated Percentage  
 Canopy Cover, and Crop Growth Stages at 11 Selected Dates for the  
 20 Winter Wheat Plots from 1978**

Calendar Date	Julian Date	Plant Height (cm)	Percentage Cover	Growth Stages	
				Numerical (after Zadoks et al., 1974)	Descriptive
04/24/78	114	35.0	54	34	stem elongation, 4th node detectable
05/01/78	121	45.2	56	35	stem elongation, 5th node detectable
05/11/78	131	70.8	66	44	booting, boots just visible
05/19/78	139	90.8	64	58	inflorescence emerges
05/25/78	145	112.0	68	64	anthesis, half-way
06/01/78	152	112.5	61	73	early milk
06/06/78	157	114.8	63	85	soft dough
06/14/78	165	115.5	64	85	soft dough
06/20/78	171	111.8	51	87	hard dough
06/23/78	174	108.5	51	89	hard dough
06/27/78	178	104.0	51	92	ready for harvest

## RESULTS AND DISCUSSION

Examples of the radiance data were plotted against Julian date (Figure 1). The red radiance vs. Julian date curve showed the influence of increasing chlorophyll absorption to ~Julian date 139 followed by a gradual decrease in chlorophyll absorption as a result of the onset of senescence (Figure 1a). The photographic infrared radiance vs. Julian date curve showed a gradual increase with time to a maximum at ~Julian date 139 followed by a decrease caused by senescence. This resulted from the direct relationship of the photographic infrared radiance to the solar density of the plant canopy (Figure 1b). The ir/red radiance ratio and the normalized difference both exhibited

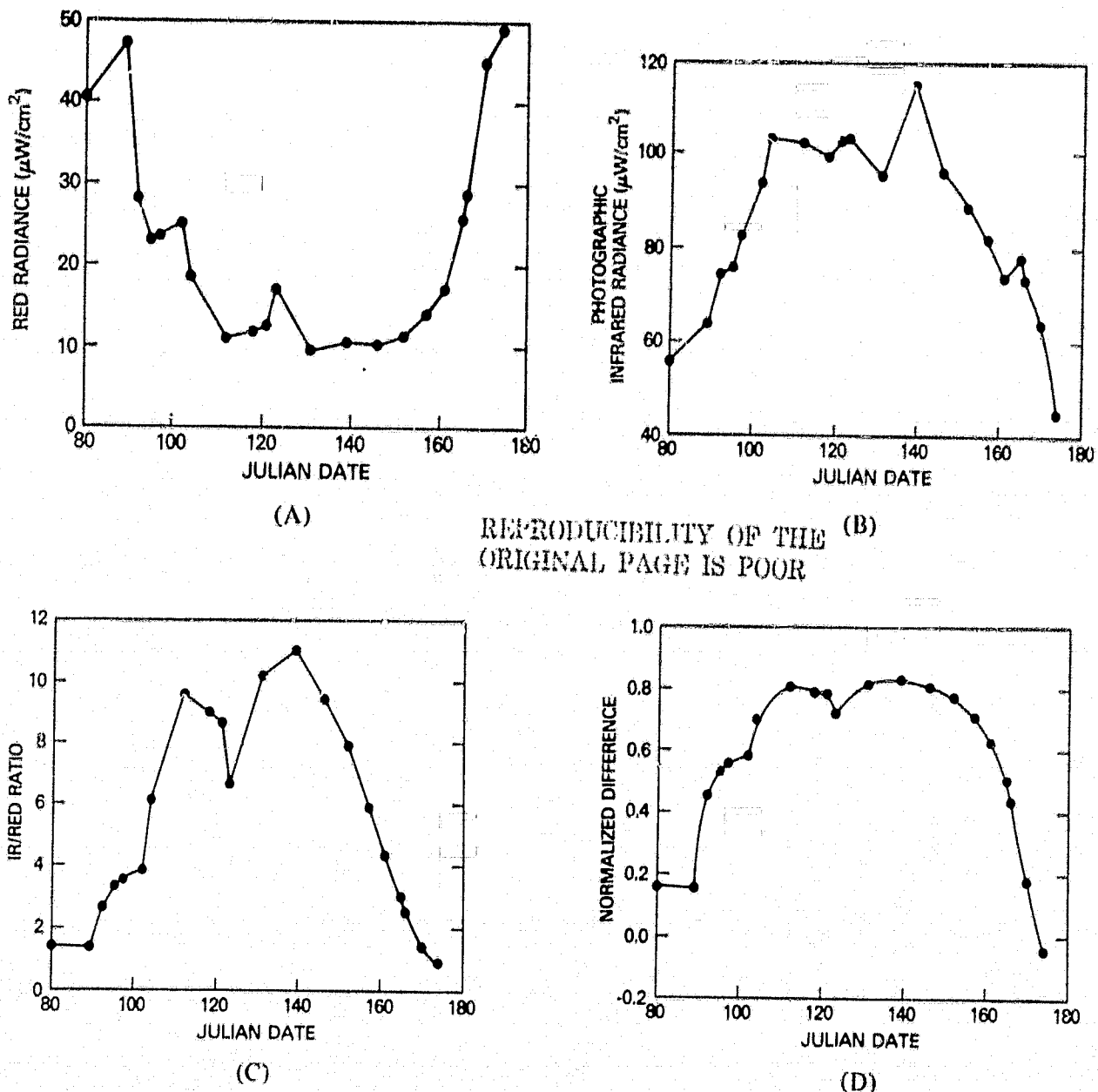
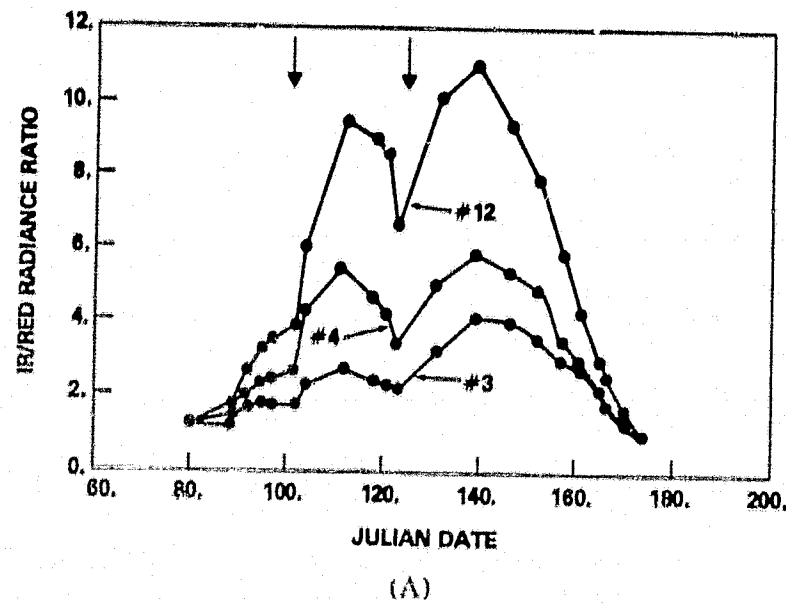


Figure 1. Red radiance, photographic infrared radiance, ir/red radiance ratio, and the normalized difference plotted against Julian date for one of 20 wheat plots sampled.  
 (A) Red radiance, (B) Photographic infrared radiance, (C) Ir/red radiance ratio, and  
 (D) Normalized difference (ND). Note how the ir/red radiance ratio and the normalized  
 difference effectively compensate for the variability in the radiance data.

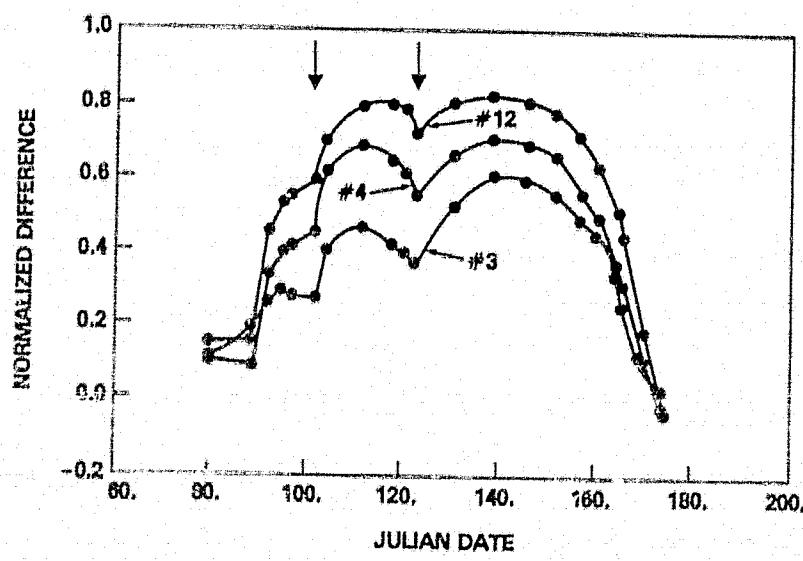
similar trends with respect to Julian date (Figures 1c and 1d, respectively). Both spectral variables showed the same five component trends with respect to Julian date: They both increased as the spring portion of the growing season began until ~Julian date 102 where their rate of increase declined; from Julian date ~102 to ~112 both showed rapid rates of increase; from Julian date ~112 to ~123 there was a decrease for both spectral variables; from Julian date ~123 to ~139 there was another increase in both spectral variables; and from Julian date ~139-175 there was the senescence caused decrease in both the ir/red radiance ratio and the normalized difference.

These same trends were observed for the majority of our experimental plots and were an example of a manifestation of transient wheat canopy water stress (Figure 2). The ir/red radiance ratio and the normalized difference both exhibited a decrease in their rate of increase by Julian date ~102. This decrease was ended by a period of rainfall on Julian date 102 which, coupled with warmer temperatures, resulted in a rapid rate of increase in the ir/red radiance ratio and normalized difference until Julian date ~112 where a period of mild drought stress again occurred, reaching maximum drought stress severity on ~Julian date 123. The later episode of drought stress was ended by a period of week-long rains which prevented any field data collection for the interval of Julian dates 125-130. The plant canopy subsequently recovered from the previous water stress condition and reached maximum values for the ir/red radiance ratio and the normalized difference on Julian date 139 which corresponded to full spike emergence (Table 2). From this date on, the progression of wheat canopy senescence resulted in a reduction of the ir/red radiance ratio and the normalized difference (Figure 2). The spectral manifestation of drought stress was consistent with previous research results (Thompson and Wehmanen, 1979; Tucker, et al., 1979c). Figure 2 also demonstrated the dynamic nature of plant canopies and how rapidly they respond to and recover from water stress conditions. We interpreted the mechanism for this spectral manifestation of plant canopy water stress to be largely due to a reduction in the leaf chlorophyll density. This followed from Figure 1a where there were decreases in red absorption (i.e., increases in radiance) for Julian dates 102 and 123 which corresponded to the episodes of water stress. The photographic infrared radiance, by contrast, did not show any effect which was attributed



(A)

REPRODUCIBILITY OF THE  
ORIGINAL PAGE IS POOR



(B)

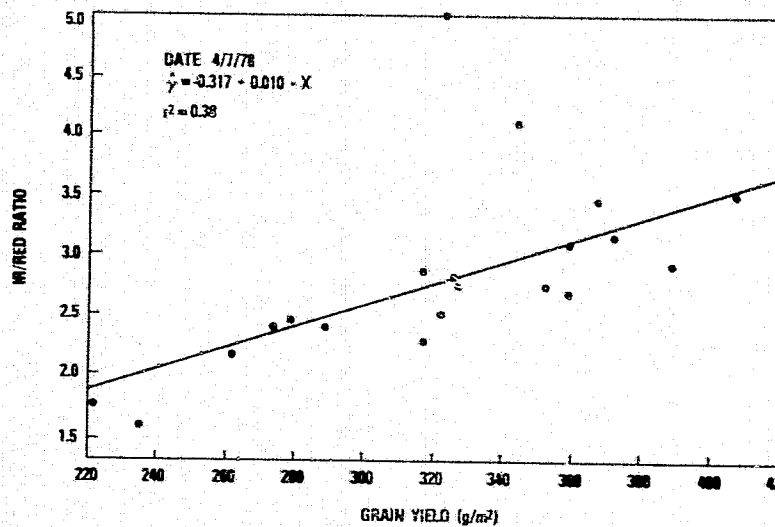
Figure 2. The ir/red radiance ratio (A) and the normalized difference (B) from three 2- x 3-m plots plotted against Julian date. The vertical arrows represent episodes of rainfall. Note the response of the two spectral variables to the occurrence of precipitation which ended periods of water stress.

to the episodes of water stress (Figure 1b). This implied that the LAI remained fairly constant while the leaf chlorophyll density was temporarily reduced, either through photooxidation, enzymatic, or some other reducing mechanism (Tucker et al., 1973; Tucker et al., 1979c).

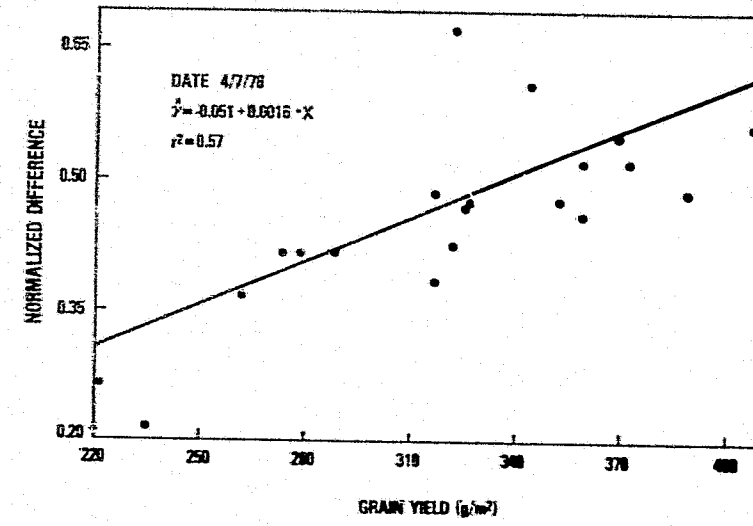
The next phase of the analysis regressed each of the 4 spectral variables against the final grain yield for each of the 21 data collection dates. Our principal attention was focussed on the ir/red ratio and the normalized difference as these linear combinations adjust for irradiational variability (Figure 3). We observed lower correlations for the first four dates, higher correlations for dates 5 and 6, and a marked decrease in correlation with grain yield for date 7 which was attributed to very windy conditions (Tables 1 and 3). Sampling dates 8, 9, and 10 were all highly correlated to grain yield. There was a slight decrease for date 11, followed by high correlations for sampling date 13 after which the correlations decreased as senescence progressed (Figure 4).

We observed a 40-day period (from Julian date 112-152) during which our spectral data were more significantly correlated to the final grain yield than earlier or later (Figure 4; Table 3). However, the regression relationships were not constant during this period, suggesting that a regional application of these relationships was doubtful (Table 4). An alternative to this was attempted in the form of integrating the spectral data in terms of Julian date or accumulated temperature units (growing degree days or equivalent). This was a remote sensing application of the leaf area duration concept.

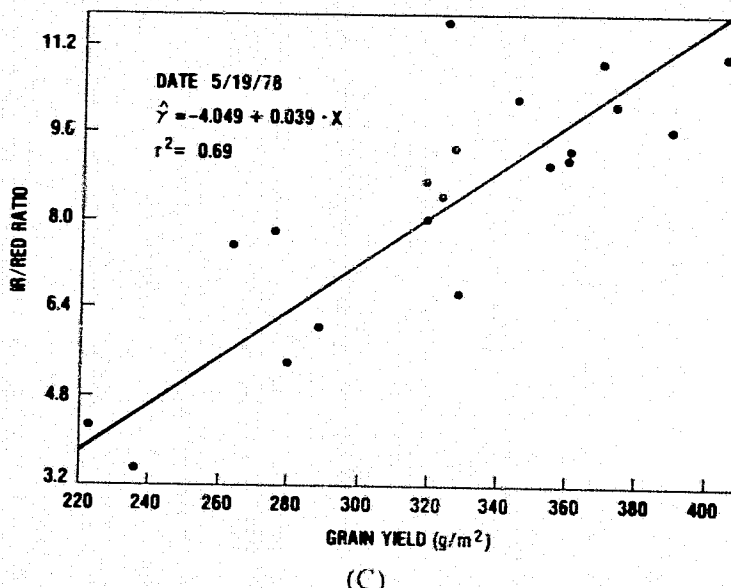
The ir/red radiance ratio and the normalized difference were integrated for four periods during the growing season: Julian dates 80-112; 112-152; 152-174; and 80-174. We observed that the plateau portion (Julian dates 112-152) of the growth curves, corresponding to the maximum green leaf biomass present, was the most highly correlated with final grain yield (Figure 5). The normalized difference spectral data from this period explained 66% of the within field variability in final grain yield while the normalized difference spectral data from the entire growing season (i.e., Julian dates 80-174) explained 64% of the same grain yield variability (Figures 5 & 6). Spectral data alone thus explained approximately two-thirds of the variability in within field grain yield. This could not be explained by meteorological models as the micro-climatic effects were largely identical for our 1.2-ha field. The earlier



(A)

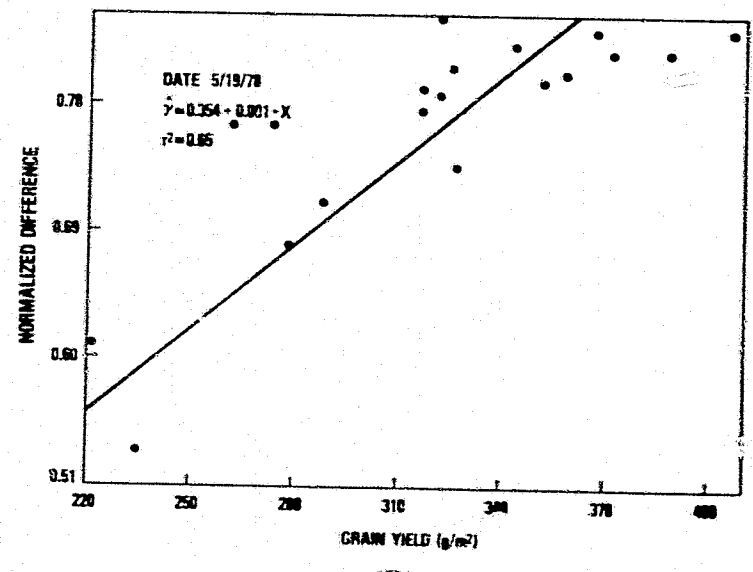


(B)



(C)

REPRODUCIBILITY OF THE  
ORIGINAL PAGE IS POOR



(D)

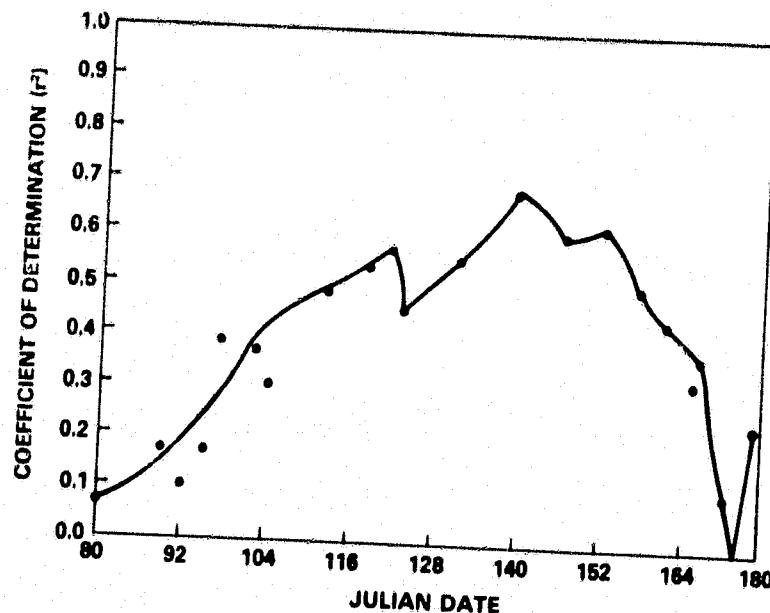
Figure 3. The ir/red radiance ratio and normalized difference plotted against grain yield for two sampling dates.

Table 3  
 Correlation Coefficients for the Four Radiance Variables and Final Grain Yield  
 for Each of the 21 Days where Spectral Data were Collected from 20 2 x 3 Plots  
 in 1978. Refer also to Figures 3 and 4.

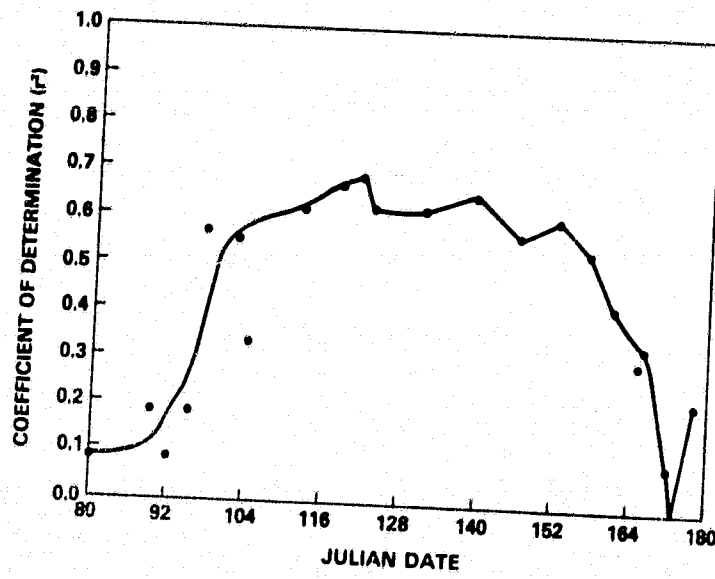
Sampling Sequence	Julian Date	Red Radiance	Ir Radiance	Ir/Red Radiance Ratio	Normalized Difference
1	80	0.14	0.51*	0.27	0.27
2	89	-0.33	0.48*	0.41	0.43
3	92	-0.22	0.42	0.31	0.30
4	95	-0.30	0.43	0.40	0.42
5	97	-0.71**	0.78**	0.62**	0.75**
6	102	-0.71**	0.80**	0.61**	0.75**
7	104	-0.51*	0.59**	0.55*	0.57**
8	112	-0.75**	0.74**	0.69**	0.78**
9	118	-0.82**	0.66**	0.73**	0.82**
10	121	-0.82**	0.54*	0.76**	0.82**
11	123	-0.78**	0.64**	0.68**	0.79**
12	131	-0.76**	0.78**	0.75**	0.78**
13	139	-0.78**	0.83**	0.83**	0.81**
14	146	-0.73**	0.76**	0.77**	0.76**
15	152	-0.78**	0.69**	0.78**	0.78**
16	157	-0.73**	0.61**	0.71**	0.73**
17	161	-0.55**	0.68**	0.66**	0.66**
18	165	-0.51*	0.49*	0.56**	0.55**
19	166	-0.57**	0.43	0.61**	0.58**
20	170	0.19	0.51*	0.32	0.30
21	174	0.46*	-0.14	-0.48*	-0.42

\*Indicates significance at the 0.05 level of probability

\*\*Indicates significance at the 0.01 level of probability



(A)

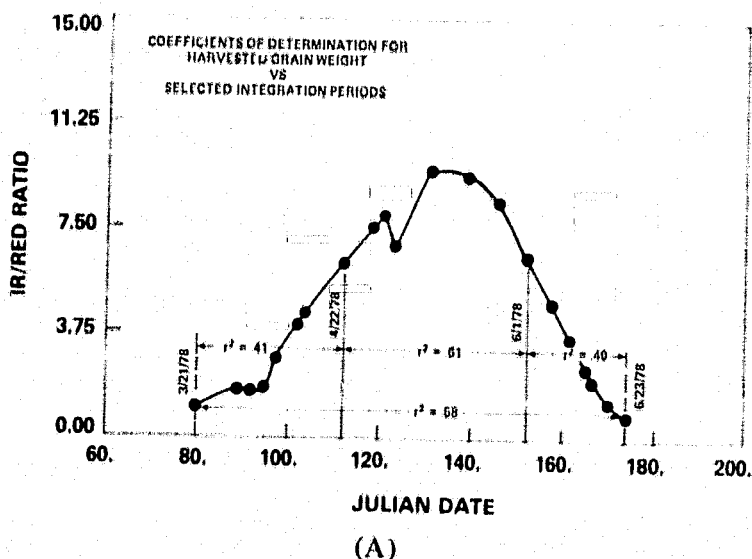


(B)

Figure 4. Coefficients of determination resulting from regressing the (A) ir/red radiance ratio or (B) normalized difference against grain yield for each of the 21 data collection dates. The  $r^2$  values presented in Figure 3 are plotted against Julian date along with the respective  $r^2$  values for the other 19 dates. Note how the normalized difference was more highly correlated with final grain yield than was the ir/red radiance ratio earlier in the growing season.

Table 4  
 Regression Derived Estimates for  $\beta_0$  and  $\beta_1$  for Julian Dates 112-152  
 Using the Ir/Red Radiance Ratio and the Normalized Difference to Predict  
 the Final Grain Yield. The Equation used was of the Form Grain Yield =  
 $\beta_0 + \beta_1$  (Spectral Variable)

Sampling Period	Julian Date	Ir/Red Radiance Ratio			Normalized Difference		
		$\beta_0$	$\beta_1$	$r^2$	$\beta_0$	$\beta_1$	$r^2$
8	112	225.6	14.7	0.48	69.1	365.0	0.61
9	118	220.9	15.3	0.53	85.1	350.3	0.67
10	121	224.4	15.0	0.57	96.6	327.0	0.68
11	123	231.5	17.2	0.46	116.8	321.1	0.62
12	131	207.7	15.0	0.56	15.8	413.7	0.61
13	139	173.1	17.8	0.69	-70.3	511.7	0.65
14	146	170.8	21.5	0.59	-26.8	475.7	0.57
15	152	148.4	29.0	0.61	-51.2	534.0	0.60



REFLECTIONS IN THIS PAPER  
ORIGINAL PAGE IS POOR

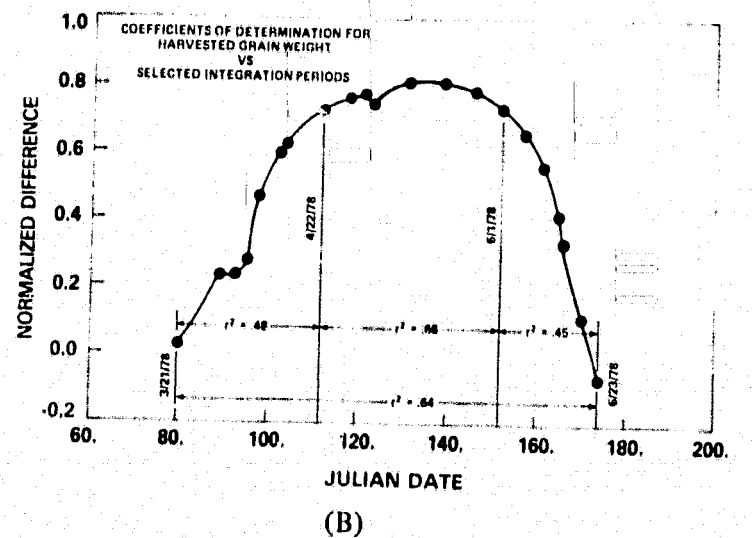


Figure 5. The  $r^2$  values resulting from the (A) ir/red radiance ratio -- Julian date and (B) normalized difference -- Julian date integrations for four different time periods: Julian dates 80-112; 112-152; 152-174; and 80-174. (Refer also to Figure 6).

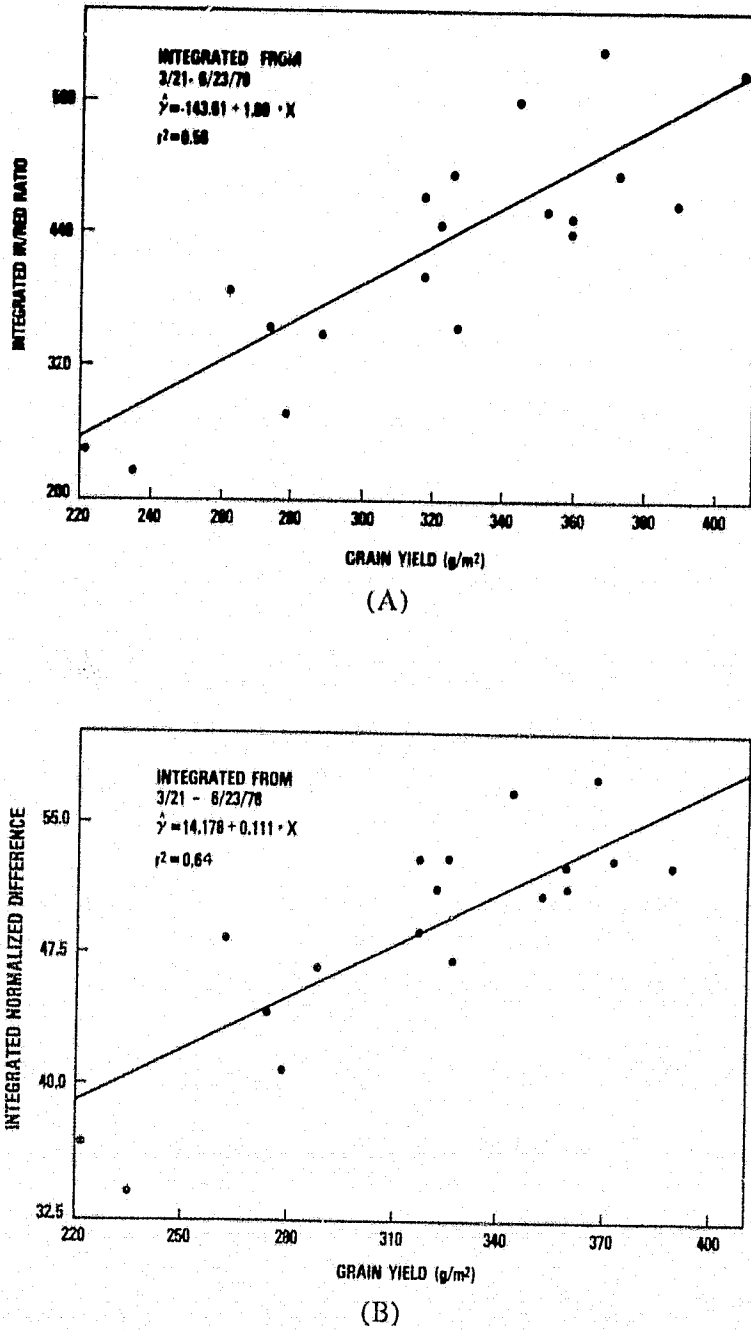


Figure 6. The relationship between the (A) ir/red radiance ratio and (B) normalized difference integrations and final grain yield for the spring portion of the growing season (Refer also to Figure 5).

integration period of Julian date 80-112 only explained 0.48% of the variability in final grain yield (Figure 5).

Any successful application of these relationships for regional remote sensing prediction of winter wheat grain yield must be able to account for within region differences in winter wheat crop phenology. From Table 4 we showed that the regression derived equation coefficients varied for the 40-day period (Julian dates 112-152) where highly significant correlations between the spectral data and final grain yield were reported (Tables 3 and 4). Thus, slight crop phenology differences within a given region would preclude the effective use of one or two satellite images obtained during this 5- to 6-week period. Either accurate crop calendar information must be available or the leaf area duration technique must be employed.

Crop calendar information is frequently lacking in extra-country situations. A possible remotely sensed substitute for this could be the combination of spectral data and accumulated temperature units (Figure 7). This follows from the basic relationship of temperature to biological activity. When combined with red and photographic infrared spectral data, representing the plant canopy vigor or potential for growth, this may have between region and/or between year comparison utility.

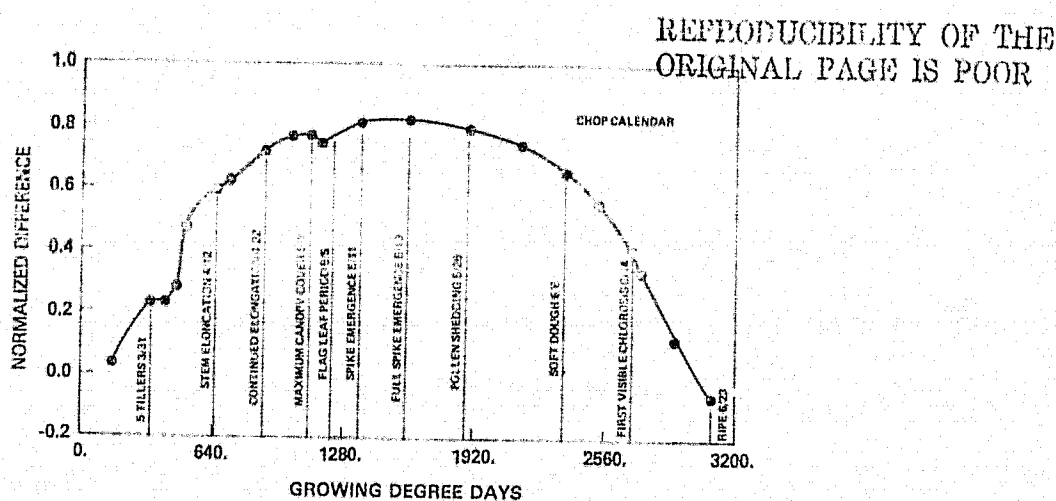


Figure 7. A possible spectral crop calendar using the normalized difference and accumulated temperature units (i.e., growing degree days).

In the event that a combination of spectral and accumulated temperature unit data would be unsatisfactory, frequent satellite coverage would be required to apply the leaf area duration concept for growing season integration of spectral data. As shown in Figure 2, frequent satellite coverage is needed to record the rapid onset of plant canopy stress conditions. It is easy to visualize the situation in Figure 2 if there were only 4, 5, or 6 data points instead of the 21 we collected. Obviously, entire stress periods might not be detected if only a few observations were available. For yield considerations, the occurrence of the stress condition is of paramount importance. If a period of water stress occurs during heading or during the grain filling period, the reduction of the grain yield is much greater than if this same stress condition occurs at some other time.

Spectral data are capable of providing large-area information highly related to crop condition or vigor. Whether these data are used in conjunction with other remotely sensed information, by simulation modelers, or by themselves, it is apparent that remotely sensed red and photographic infrared spectral data can supply valuable crop condition information.

## CONCLUSIONS

1. Frequently collected spectral data were shown to be highly related to crop condition. Two periods of water stress were readily apparent.
2. A 40-day period existed from the beginning of stem elongation through antheses during which the spectral data were highly correlated with final grain yield and explained at least 60% of the variability.
3. The integrated spectral data explained 64% of the variability in within field final grain yield. This could not be explained using meteorological models as the micro-climate conditions were very similar for our experimental wheat field.
4. Large-scale extra-country application for our findings would require a spectral crop calendar. We propose a possible spectral-accumulated temperature unit crop calendar. If this is not feasible, we suggest frequent satellite observations and application of the leaf area duration concept.
5. The combination of spectral data and other environmental or agronomic data will improve the predictive utility of yield forecasting. While spectral data are useful by themselves, they are more useful in combination with other types of data.

## ACKNOWLEDGMENTS

We thank Paul Pinter, Jr., Ray Jackson, John Colwell, and Wayne Willis for encouragement and suggestions on the manuscript. We thank the following people for help in the collection of data in the field: Chris Justice, Dan Kimes, Donna Strahan, Diana Crowley, Maryann Karineh, Charley Walther, Josette Pastor, Jelle Helkima, Steve Bogash, Don Friedman, Bill Jones and Bill Wigton. We thank Freeman Smith for the loan of the instrument.

RECEIVED ON THE  
ORIGINAL DATE

## REFERENCES

- Colwell, J. E., D. P. Rice and R. F. Nalpeka. 1977. Wheat yield forecasts using Landsat data. In Proc. of the 11th International Symposium on Remote Sensing of Environment. Univ. of Michigan, Ann Arbor, p. 1245-1254.
- Deering, D. W., J. W. Rouse, R. H. Haas, and J. A. Schell. 1975. Measuring forage production of grazing units from Landsat MSS data. Proc. of the 10th International Symposium on Remote Sensing of Environment, pp. 1169-1178.
- EarthSat Corp. 1976. EarthSat spring wheat yield system test. Final Report, Washington, DC
- Harlan, J. C. and S. Liu. 1975. A one year, one site Landsat study for determination of unharvested winter wheat acreage. Tech Report RSC-66, Remote Sensing Center, Texas A&M Univ., College Station.
- Hammond, A. L. 1975. Crop forecasting from space: Toward a global food watch. Science, 188: 434-436.
- Heilman, J. L., E. T. Kanemasu, J. O. Bagley, and V. P. Rasmussen. 1977. Evaluating soil moisture and yield of winter wheat in the Great Plains using Landsat data. Remote Sensing of Environment, 6: 315-326.
- Idso, S. B., R. D. Jackson, and R. J. Reginato. 1977a. Remote sensing of crop yields. Science, 196: 19-25.
- Idso, S. B., R. D. Jackson, and R. J. Reginato. 1976b. Albedo measurements as a technique for the remote sensing of crop yields. Nature, 266: 625-628.
- Kanemasu, E. T., J. L. Heilman, J. O. Bagley, and W. L. Powers. 1977. Using Landsat data to estimate evapotranspiration of winter wheat. Environ. Management 2(6):515-520.
- LACIE. 1978. Briefing materials for technical presentations. the LACIE Symposium, NASA/JSC, Vol. B.
- MacDonald, R. B., and F. G. Hall, 1977. LACIE: A look to the future. In Proc. of the 11th International Symposium on Remote Sensing of Environment. Univ. of Michigan, Ann Arbor, p. 429-465.

- Morain, S. A., and D. L. Williams. 1975. Wheat production estimates using satellite images. *Agron. J.*, 67: 361-364.
- Pearson, R. L., L. D. Miller, and C. J. Tucker. 1976. Hand-held radiometer to estimate gramineous biomass. *Appl. Opt.* 15 (2): 416-418.
- Richardson, A. J., C. L. Wiegand, J. F. Arken, P. R. Nixon, and A. H. Gerberman. 1979. Spectral indicators of sorghum development and their implications for growth modeling. To be submitted to *Photogram. Engr. and Remote Sensing*.
- Rouse, J. W., R. H. Haas, J. A. Schell, and D. W. Deering. 1973. Monitoring vegetation systems in the Great Plains with ERTS. Third Symposium on Significant Results Obtained with ERTS-1. NASA SP-351: 309-317.
- Thompson, D. R. and O. A. Wehmanen. 1979. Using Landsat digital data to detect moisture stress. *Photogram. Engr. and Remote Sensing* 45 (2): 201-207.
- Tucker, C. J. 1979. Red and photographic infrared linear combinations for monitoring vegetations. *Remote Sensing of Environment* 8(2):127-150.
- Tucker, C. J., L. D. Miller, and R. L. Pearson. 1973. Measurement of the combined effect of green biomass, chlorophyll, and leaf water on canopy spectro-reflectance of the short-grass prairie. Proc. of the 2nd Annual Remote Sensing of Earth Resources Conf., Space Inst. of Tenn. Univ., pp. 601-627.
- Tucker, C. J., J. H. Elgin, Jr., and J. E. McMurtrey, III. 1979a. Temporal spectral measurements of corn and soybean crops. *Photogram. Engr. and Remote Sensing* 45(5): 600-608.
- Tucker, C. J., J. H. Elgin, Jr., J. E. McMurtrey, III and C. J. Fan. 1979b. Monitoring corn and soybean crop development with hand-held radiometer spectral data. *Remote Sensing of Environment* (in press).
- Tucker, C. J., J. H. Elgin, Jr., and J. E. McMurtrey, III. 1979c. Relationship of red and photographic infrared spectral radiances to alfalfa biomass, forage water content, percentage canopy cover, and severity of drought stress. Submitted to *Remote Sensing of Environment*.

- Tucker, C. J., B. N. Holben, J. H. Elgin, Jr., and J. E. McMurtrey, III. 1979d. Remote sensing of winter wheat total dry matter accumulation. To be submitted to *Science*.
- Wiegand, C. L., A. J. Richardson, and E. T. Kanemasu. 1979. Leaf area index estimates for wheat from Landsat and their implications for evapotranspiration and crop modeling. *Agron. J.* 71: 336-342.
- Zadoks, J. C., T. T. Chang, and C. F. Konzak. 1974. A decimal code for the growth stages of cereals. *Weed Research* 14:415-421.

## BIBLIOGRAPHIC DATA SHEET

1. Report No. TM-80318	2. Government Accession No.	3. Recipient's Catalog No.		
4. Title and Subtitle The Relationship of Red and Photographic Infrared Spectral Data to Grain Yield Variation within a Winter Wheat Field		5. Report Date		
7. Author(s) C. J. Tucker et al.		6. Performing Organization Code		
9. Performing Organization Name and Address Earth Resources Branch NASA/GSFC Greenbelt, Maryland 20771 USA		8. Performing Organization Report No.		
12. Sponsoring Agency Name and Address Earth Resources Branch NASA/GSFC Greenbelt, Maryland 20771 USA		10. Work Unit No.		
		11. Contract or Grant No.		
		13. Type of Report and Period Covered		
		14. Sponsoring Agency Code		
15. Supplementary Notes None				
16. Abstract <p>Two-band hand-held radiometer data from a winter wheat field, collected on 21 dates during the spring growing season, were correlated within field final grain yield. Significant linear relationships were found between various combinations of the red and photographic infrared radiance data collected and the grain yield. The spectral data explained ~64% of the within field grain yield variation. This variation in grain yield could not be explained using meteorological data as these were similar for all areas of the wheat field. Most importantly, data collected early in the spring were highly correlated with grain yield, a five-week time window existed from stem elongation through antheses in which the spectral data were most highly correlated with grain yield, and manifestations of wheat canopy water stress were readily apparent in the spectral data.</p>				
17. Key Words (Selected by Author(s)) remote sensing, vegetation, monitoring, yield estimation, stress detection		18. Distribution Statement		
19. Security Classif. (of this report)		20. Security Classif. (of this page)	21. No. of Pages	22. Price*